学 術
Arts and Sciences
ノート

# The optimal scanning method for three-dimensional $T_1$-weighted black-blood turbo spin-echo MRI in the aortic arch

*大動脈弓部を対象とした3D $T_1$-weighted black-blood turbo spin-echo MRI法の最適化*

Kenichi Nakagawa[1)], Masanori Kinosada (medical doctor)[2)], Takashi Tabuchi[3)], Noriyoshi Morimoto[1)], Sachi Fukushima[1)], Takashi Ogasahara[1)], Masayuki Kumashiro[1)]

1) Department of Radiological Technology, Kurashiki Central Hospital
2) Department of Neurosurgery, Kurashiki Central Hospital
3) Department of Medical Technology, Kurashiki Central Hospital

**Key words:** aortic arch, black blood, plaque, aortogenic embolism, TEE

【Abstract】

Aortic arch plaques visualized using transesophageal echocardiography (TEE) are at risk for brain embolism. However, TEE is not suitable for all patients. Therefore, we focused on scan of MRI with $T_1$-weighted ($T_1$w) black blood turbo spin-echo (TSE) imaging. This study aimed to clarify the optimal scanning method for 3D $T_1$w black-blood TSE imaging in the aortic arch. Five healthy volunteers (mean age, 33.8 years; range, 25.0 to 57.0 years) participated in this study. We obtained Institutional Review Board approval and the informed consent of all subjects. All experiments were acquired by volume isotropic TSE acquisition (VISTA) with anti-DRIVE using a 1.5-T magnetic resonance scanner. The study protocol was divided on the basis of two aims: 1) To evaluate the combinations of six patterns of phase direction with and without electrocardiography (ECG) and navigator echo, and 2) to compare the ECG during systole and diastole to determine the optimal trigger timing. We determined that the combination of phase direction foot-head (FH), ECG, and navigator echo was the best scanning method. Furthermore, the optimal trigger timing was during diastole, which showed lesser movement of the vessel wall than during systole. Our results suggest that 3D $T_1$W BB-TSE with anti-DRIVE using the diastolic trigger timing by ECG-gating and navigator echo respiratory gating in the aortic arch can provide beneficial information for clinical practice.

**【要 旨】**

経食道心エコー図検査（TEE）で検出される大動脈弓部プラークは，脳梗塞を引き起こす原因となる．しかし，TEEは全ての患者に適用できる検査ではない．そこで$T_1$強調BB TSEによるMRIの撮像に着目した．本研究の目的は，大動脈弓部に対する3D-$T_1$強調BB TSEの撮像条件の最適化である．本研究は健常ボランティア5人を対象とし，全て倫理委員会の承認と同意を得られている．検討項目は1）位相方向・心電図同期・navigator echoの組み合わせによる評価と2）心電図同期のタイミングについて評価した．最適な撮像条件は，位相方向FH，心電図同期（拡張期）およびnavigator echoを併用することであった．

07

## 1. Introduction

Complex atherosclerotic plaques include irregular surface plaques, ulcerated plaques, and mobile plaques [1), 2)]. Complex plaques that are observed in the aortic arch on transesophageal echocardiography (TEE) are at high risk for aortogenic brain embolism [3)-8)]. However, TEE, which is associated with a number of complications and contraindications, is not suitable for all patients [9)].

中河 賢一[1)]，紀之定 昌則[2)]，田渕　隆[3)]，森本 規義[1)]
福島 沙知[1)]，小笠原 貴史[1)]，熊代 正行[1)]

1）倉敷中央病院　放射線技術部
2）倉敷中央病院　脳神経外科（医師）
3）倉敷中央病院　医療技術部

Received December 25, 2017; accepted November 30, 2018

However, in the examination of carotid plaques, magnetic resonance imaging (MRI) can be used for the diagnosis of plaque components based on MR contrast [10), 11)]. Unstable carotid plaques are characterized by a fibrous cap, atheroma, and intraplaque hemorrhage. In addition, high-intensity plaques on $T_1$-weighted black blood ($T_1$W BB) MRI are considered a useful finding in assessing unstable plaques [12)-14)].

Therefore, we focused on the black blood image of MRI as an adjunct diagnostic modality for complex plaques of the aortic arch that are difficult to observe owing to multiple artifacts. To address these problems, we devised a scanning methodology using three-dimensional $T_1$-weighted black-blood turbo spin-echo (3D $T_1$W BB-TSE) MRI in the aortic arch. The aim of this study was to clarify the optimal scanning method for 3D $T_1$W BB-TSE.

## 2. Materials and Methods

### 2.1 Patients

Five healthy volunteers (mean age, 33.8 years; range, 25.0 to 57.0) participated in this study. We obtained Institutional Review Board approval and informed consent from all participants.

### 2.2 MR imaging protocol

All scans were performed on a 1.5-Tesla MR scanner (Ingenia R5-2; Philips Healthcare, Best, The Netherlands) using a 15-channel ds Torso coil as the receiver. All experiments were acquired by volume isotropic TSE acquisition (VISTA) with anti-driven-equilibrium post-pulse (anti-DRIVE) [15), 16)]. The parameters for VISTA with anti-DRIVE were as follows: repetition time (TR), 1 beat; echo time (TE), 24 ms; field of view (FOV), 260*260*70 mm; acquisition matrix, 1.1*1.1*4 mm; reconstruction matrix, 0.55*0.55*2 mm; refocusing flip angle, 30°; TSE factor, 25; start up echo, 4; number of signals averaged (NSA), 1. The fat saturation pulse used spectral attenuated inversion recovery (SPAIR).

### 2.3 Study protocol and analysis

We obtained 3D $T_1$W BB-TSE images in volunteers who were asked to maintain a natural breathing style while undergoing oblique sagittal scans of the aortic arch. The study protocol consisted of two processes: first, to evaluate the combination of six patterns for phase direction anterior-posterior or foot-head (AP or FH), with and without electrocardiogram-gating (ECG-gating) and navigator echo; and then, to compare ECG-gating during systole and diastole to determine the optimal trigger timing.

Two radiological technologists had experience, more than 5 years in MRI division, and were involved in visually ranking of motion artifacts for six image patterns of phase direction. The results of the visual evaluation were converted into normal scores, and analysis by the least significant difference (LSD) method was performed on this result, and significant differences in ranking were examined [17)]. The P-value for significant difference was defined as $P<0.05$.

## 3. Results

Figure 1 shows the results of a visual evaluation performed using the normalized-rank method and the images obtained using six

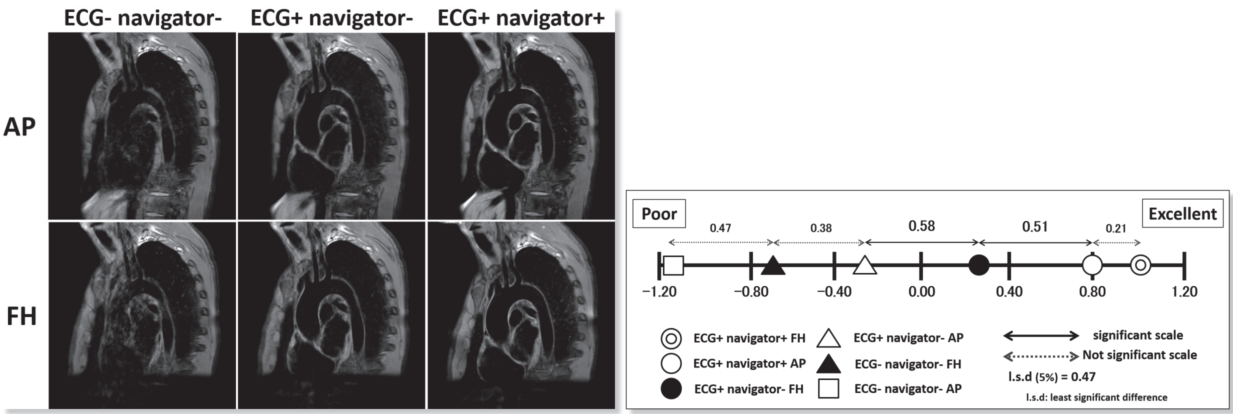


Fig.1 The anterior-posterior: AP (top row) and foot-head: FH (bottom row) phase direction. A comparison of three-dimensional $T_1$-weighted black-blood turbo spin-echo images obtained from the electrocardiography (ECG)- navigator-, ECG+ navigator-, and ECG+ navigator+ scans, respectively, are shown. Also shown are the results of the visual evaluation evaluated using the normalized-rank method.

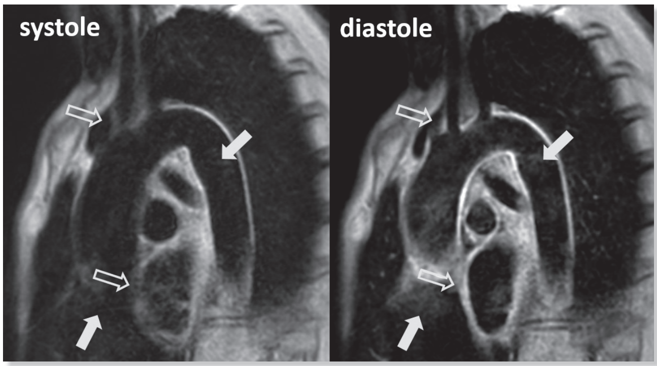


Fig.2 Comparison of the systolic images and the diastolic images obtained using navigator echo. The open arrow shows the movement of the vessel wall, and the closed arrow shows the black blood effect.

patterns of phase direction (AP or FH), with and without ECG-gating and navigator echo. A significant difference between ECG+navigator-FH and ECG+navigator-AP suggested that FH improved the motion artifacts (LSD, $P<0.05$). Moreover, differences of image qualities between ECG+navigator+FH and ECG+navigator-FH, or ECG+navigator+AP and ECG+navigator-AP indicated usefulness of navigator echo. Furthermore, ECG-gating also improved the motion artifacts between ECG+navigator-FH and ECG-navigator-FH.

Further, Figure 2 shows the images obtained using ECG-gating on systole and diastole with navigator echo. ECG-gating on systole had a profound effect on both BB and motion artifacts of the ascending aorta. In contrast, low extent of flow-related signal loss was observed on ECG-gating at diastole, but motion artifacts of the vessel walls were decreased. The images from the four remaining healthy volunteers demonstrated the same results.

## 4. Discussion

### 4.1 The effect of respiration

In this study, the use of navigator echo improved the image quality by reducing the motion artifacts associated with respiration (Figure 1). Navigator echo measured the diaphragm position during free breathing, and this information allowed for triggering on the defined window within the respiratory cycle. Ample studies have demonstrated the utility of navigator echo [18]. However, it is necessary to set standards high to reduce the effect of respiration, thereby scan time is extended. In addition, oblique sagittal scanning could be problematic in image qualities because of motion artifact in the liver and the thorax. The AP and FH phase directions would reduce the motion artifact by the liver and the thorax, respectively. This study demonstrated that the FH phase direction resulted in improvement of the image quality. Setting the navigator echo around the diaphragm also improved the precision of the image of the liver without motion artifact of the liver. However, we assume that the accuracy of movement correction of the thorax was reduced due to the navigator echo directly collection at a site distant from the thorax. In other words, modifications to the setup the navigator echo would be required to decrease motion artifact of the thorax on imaging of the aortic arch.

### 4.2 The effect of ECG-gating

In this study, we were able to obtain good image qualities by reducing the motion artifacts associated with pulsations with ECG-gating. Furthermore, significant results were obtained for visual evaluation performed using the normalized-rank method as in Figure 1. The aortic arch generally shows severe artifacts owing to pulsations of the aortic arch [19]. However, the present results indicated that ECG-gating reduced the motion artifact of the pulsations because of synchronization with the cardiac phase. We compared the effect of setting the cardiac trigger timing to either systole or diastole. Figure 2 shows the relationship between the BB effect and the motion artifact of the ascending aorta. For the patients with reduced blood flow, the timing of ECG-gating at systole was better than diastole because of the flow void effect. In other words, regarding the BB effect, the systole is more advantageous. However, several studies have reported that mobile or ulcerated plaques and large atheromatous aortic plaques of over 4 mm in thickness on TEE can cause aortgenic brain embolism [4)-6)]. Therefore, to diagnose complex plaques in the aortic arch, a reliable method for measuring the thickness of the aortic plaques was important. Thus, the reduction of motion artifacts should be given priority over the BB effect in diagnosis of complex plaques in the aortic arch. The images in Figure 2 suggest that ECG-gating during diastole was more accurate.

### 4.3 Clinical images and Limitations

Figure 3 shows the clinical images of the aortic arch. We were able to obtain the high intensity plaques of the aortic arch. Furthermore, 3D $T_1$W BB-TSE with anti-DRIVE shows more clearly existences of multiple vulnerable plaques on the vessel wall comparing with contrast-enhanced computed tomography. However, for the patient with cardiac hypofunction or a reduced blood flow, the diastolic image might decrease the contrast of complex plaques and the BB effect, increasing possibility of incorrect diagnosis. In addition, the measurement of thickness of vessel wall in the patient with arrhythmia using this method would not shows high accuracy of images.

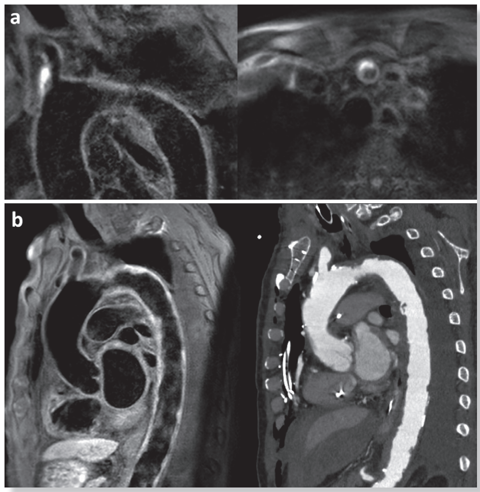


Fig.3 Clinical images of 3D $T_1$W black blood-TSE with anti-driven-equilibrium post-pulse (3D $T_1$W BB-TSE with anti-DRIVE) in the aortic arch when using the diastolic trigger timing with ECG-gating and navigator echo respiratory gating. On 3D $T_1$W BB-TSE with anti-DRIVE (a), the high intensity plaque of brachiocephalic artery is seen. A comparison between 3D $T_1$W BB-TSE with anti-DRIVE and contrast-enhanced computed tomography (CECT) (b), 3D $T_1$W BB-TSE with anti-DRIVE shows multiple vulnerable plaques on the vessel wall more clearly than CECT.

## 5. Conclusion

Our results suggest that 3D $T_1$W BB-TSE with anti-driven-equilibrium post-pulse in the aortic arch could provide beneficial information for clinical practice when using the diastolic trigger timing with ECG-gating and navigator echo respiratory gating.


## Acknowledgements

We sincerely thank the RTs in the Department of Radiological Technology, Kurashiki Central Hospital.

### Conflict of interest

The authors declare that they have no conflict of interest.

## 図の説明

Fig.1 上段は位相方向APと下段は位相方向FH．それぞれ3D $T_1$強調black-blood TSEのECG- navigator-，ECG+ navigator-，ECG+ navigator+の画像を示す．また正規化順位法による視覚評価の結果も示す．

Fig.2 navigator echoを使用して得られた収縮期と拡張期画像を比較する．開矢印は血管壁の動きを，閉矢印はblack blood効果を示す．

Fig.3 大動脈弓部を対象としたnavigator echoによる呼吸補正と拡張期のタイミングによる心電図同期を併用した3D $T_1$W BB-TSE with anti-DRIVEの臨床画像．3D $T_1$W BB-TSE with anti-DRIVEは腕頭動脈に高信号のプラークが描出されている（a）．3D $T_1$W BB-TSE with anti-DRIVEと造影CTの比較で，造影CTよりも3D $T_1$W BB-TSE with anti-DRIVEの方が明瞭に多数の不安定プラークを描出している（b）．

## References

1） Di Tullio MR, Sacco RL, et al.: Aortic atheromas and acute ischemic stroke: a transesophageal echocardiographic study in an ethnically mixed population. Neurology, 46, 1560-1566, 1996.
2） Di Tullio MR, et al.: Aortic atheroma morphology and the risk of ischemic stroke in a multiethnic population. Am Heart J, 139, 329-336, 2000.
3） Shimada Y, et al.: Aging, aortic arch calcification, and multiple brain infarcts are associated with aortogenic brain embolism. Cerebrovascular diseases, 35 (3), 282-290, 2013.
4） Okuzumi A, et al.: Impact of low-density lipoprotein to high-density lipoprotein ratio on aortic arch atherosclerosis in unexplained stroke. Journal of the Neurological Sciences, 326, 83-88, 2013.
5） Aortogenic embolism and paradoxical embolism due to patent foramen ovale and deep vein thrombosis. Japanese Journal of Neurosurgery, 17 (12), 901-908, 2008.
6） Amarenco P, et al.: Atherosclerotic disease of the aortic arch and the risk of ischemic stroke. N Engl J MED, 331, 1474-1479, 1994.
7） Sugioka K, et al.: Relationship between complex plaques detected by vascular ultrasound and plaque destabilization. Jpn J Med Ultrasonics, 37 (4), 455-462, 2010.
8） Kaneko K, et al.: The presence of the non-calcified plaques in the aortic arch closely contribute to the recurrence of atherothrombotic cerebral infarction. Shinzo, 40 (1), 24-33, 2008.
9） Exploration for Embolic Sources by Transesophageal Echo Cardiography. Neurosonology, 19 (3), 132-146, 2006.
10） Watanabe Y, et al.: MR plaque imaging of the carotid artery. Neuroradiology, 52, 253-274, 2010.
11） Yoshida Y, et al.: Characterization of Carotid Atherosclerosis and Detection of Soft Plaque with Use of Black-Blood MR Imaging. AJNR Am J Neuroradiol, 29, 868-874, 2008.
12） Horie T, et al.: Improved visualization of long-axis black-blood imaging of the carotid arteries using phase sensitive inversion recovery combined with 3D IR-$T_1$TFE. Japanese Journal of Radiological Technology, 67 (8), 888-894, 2011.
13） Nakamura M, et al.: Volumetric black blood angiography by low refocusing flip angle 3D turbo spin echo in the intracranial vertebrobasilar artery. JJMRM, 31 (4), 187-197, 2011.
14） Nakagawa K, et al.: Optimization of black blood cine for mobile plaque. Japanese Journal of Radiological Technology, 69 (11), 1274-1280, 2013.
15） Ogawa M, et al.: Fundamental study of three-dimensional fast spin-echo imaging with spoiled equilibrium pulse. Japanese Journal of Radiological Technology, 73 (1), 26-32, 2017.
16） Yoneyama M, et al.: Improvement of $T_1$ Contrast in Whole-brain Black-blood Imaging using Motion-sensitized Driven-equilibrium Prepared 3D Turbo Spin Echo (3D MSDE-TSE). Magn Reson Med Sci, 13 (1), 61-65, 2014.
17） Nakamae M.: Study of the Reliability of Visual Evaluation by the Ranking Method: Analysis of Ordinal Scale and Psychological Scaling Using the Normalized-rank Approach. Japanese Journal of Radiological Technology, 56 (5), 725-730, 2000.
18） Wang Y, et al.: Navigator-echo-based real-time respiratory gating and trigger for reduction of respiration effects in three-dimensional coronary MR angiography. Radiology, 198 (1), 55-60,1996.
19） Jonathan SL, et al.: Three-dimensional time-of-flight MR Angiography; Applications in the abdomen and thorax. Radiology, 179, 261-264, 1991.